T. Bierkandt, M. Höner, N. Gaiser, N. Hansen, M. Köhler, T. Kasper, Experimental flat flame study of monoterpenes: Insights into the combustion kinetics of α-pinene, β-pinene, and myrcene, Proceedings of the Combustion Institute 38 (2021) 2431-2440.

https://doi.org/10.1016/j.proci.2020.06.204

# Experimental flat flame study of monoterpenes: Insights into the combustion kinetics of α-pinene, β-pinene, and myrcene

Thomas Bierkandt[1,*], Martin Höner[2], Nina Gaiser[1], Nils Hansen[3], Markus Köhler[1], and Tina Kasper[2]

[1]Institute of Combustion Technology, German Aerospace Center (DLR), Pfaffenwaldring 38-40, 70569 Stuttgart, Germany

[2]Mass Spectrometry in Reactive Flows, IVG, University of Duisburg-Essen, 47057 Duisburg, Germany

[3]Combustion Research Facility, Sandia National Laboratories, Livermore CA 94550, USA

*Corresponding Author: Thomas Bierkandt, German Aerospace Center, Pfaffenwaldring 38-40, 70569
Stuttgart, Germany
Phone: +49-711-6862-8178, Fax: +49-711-6862-578
E-mail: thomas.bierkandt@dlr.de

**Colloquium Topic Area: Laminar Flames or Reaction Kinetics (alternative session)**

Word count method: WYSIWYG word processor

| Part | Method | # words |
|---|---|---|
| Abstract | Microsoft Word 2010 word count | 281 |
| Main text | Microsoft Word 2010 word count | 4231 |
| Introduction | | 686 |
| Experiment | | 258 |
| Results | | 2779 |
| Conclusions | | 383 |
| Acknowledgments | | 125 |
| Equations | No equations | 0 |
| Nomenclature | No nomenclature | 0 |
| References | (42 + 2) × 2.3 lines/ref × 7.6 words/line | 769 |
| Tables | No tables | 0 |
| Figure 1 | [(63.8 mm + 10 mm) × 2.2 words/mm × 1] + 14 | 176 |
| Figure 2 | [(55.0 mm + 10 mm) × 2.2 words/mm × 1] + 23 | 166 |
| Figure 3 | [(44.4 mm + 10 mm) × 2.2 words/mm × 1] + 29 | 149 |
| Figure 4 | [(56.2 mm + 10 mm) × 2.2 words/mm × 1] + 15 | 161 |
| Figure 5 | [(55.8 mm + 10 mm) × 2.2 words/mm × 1] + 30 | 175 |
| Figure 6 | [(81.2 mm + 10 mm) × 2.2 words/mm × 1] + 10 | 211 |
| Figure 7 | [(55.9 mm + 10 mm) × 2.2 words/mm × 1] + 15 | 160 |
| **Total (excl. abstract)** | | **6198** |

Supplementary Material has been included in the submission of this paper

Submitted to the 38th International Symposium on Combustion, Adelaide, 2020

Color figures in electronic version only

## Abstract

Pinenes and pinene dimers have similar energy densities to petroleum-based fuels and are regarded as alternative fuels. The pyrolysis of the pinenes is well studied, but information on their combustion kinetics is limited. Three stoichiometric, flat premixed flames of the $C_{10}H_{16}$ monoterpenes α-pinene, β-pinene, and myrcene were investigated by synchrotron-based photoionization molecular-beam mass spectrometry (PI-MBMS) at the Advanced Light Source (ALS). This technique allows isomer-resolved identification and quantification of the flame species formed during the combustion process. Flame-sampling molecular-beam mass spectrometry even enables the detection of very reactive radical species. Myrcene was chosen because of its known formation during β-pinene pyrolysis. The quantitative speciation data and the discussed decomposition steps of the fuels provide important information for the development of future chemical kinetic reaction mechanisms concerning pinene combustion. The main decomposition of myrcene starts with the unimolecular cleavage of the carbon-carbon single bond between the two allylic carbon atoms. Further decompositions by β-scission to stable combustion intermediates such as isoprene ($C_5H_8$), 1,2,3-butatriene ($C_4H_4$) or allene ($aC_3H_4$) are consistent with the observed species pool. Concentrations of all detected hydrocarbons in the β-pinene flame are closer to the myrcene flame than to the α-pinene flame. These similarities and the direct identification of myrcene by its photoionization efficiency spectrum during β-pinene combustion indicate that β-pinene undergoes isomerization to myrcene under the studied flame conditions. Aromatic species such as phenylacetylene ($C_8H_6$), styrene ($C_8H_8$), xylenes ($C_8H_{10}$), and indene ($C_9H_8$) could be clearly identified and have higher concentrations in the α-pinene flame. Conclusively, a higher sooting tendency can generally be expected for this monoterpene. The presented quantitative speciation data of flat premixed flames of the three monoterpenes α-pinene, β-pinene, and myrcene give insights into their combustion kinetics.

**Keywords:** Monoterpene; Pinene; Biofuel, Photoionization; Molecular-beam mass spectrometry

## 1. Introduction

Over the past 25 years, the global production of biofuels as an alternative to fossil fuels for the transport sector has continuously increased [1] as they enable a reduction of $CO_2$ emissions and other harmful pollutants. The stringent requirements for aviation fuels, e.g., a high energy density and a low freezing point [2], typically restrict the direct use of conventional biofuels as an alternative to petrol-based aviation fuels. Currently commercially available biojet fuels, e.g., hydroprocessed esters and fatty acids (HEFA) or farnesane, are suitable as drop-in components for Jet A-1 used in civil aviation, while alternatives to petroleum-based fuels with even higher energy densities for power-intensive aircraft, rockets, and missiles are limited. For such applications, the pinene dimers, which have a similar energy density to the tactical fuel JP-10, could be a promising alternative [3,4]. Hydrogenated pinene dimers ($C_{20}H_{34}$) were synthesized in high yield by dimerization of β-pinene and subsequent hydrogenation over $PtO_2$ during chemical catalysis [3]. Highest yields of more than 90% were reached with Nafion as catalyst and a reaction time of six hours at 100°C and atmospheric pressure [3]. Meylemans et al. have also synthesized hydrogenated terpene dimers as potential high energy density fuels from α-pinene, two other terpenes, and turpentine by selective dimerization and subsequent hydrogenation [4]. The high viscosity of such terpene dimers prevents their use as single fuel component, but 50:50 blends with conventional fuels, e.g., JP-8 and JP-10, have acceptable viscosity even at lower temperatures [5]. A promising method for obtaining pinenes as precursors for pinene dimers from readily accessible raw materials is the synthesis of pinenes from conversion of glucose by engineered *Escherichia coli* bacteria [6]. Currently, the yield is low, e.g., Sarria et al. have achieved 1.2% of the technically possible yield, and has to increase to at least 26% to be an economical alternative to JP-10 [6].

Pinenes ($C_{10}H_{16}$) are unsaturated, bicyclic compounds and belong to the class of terpenes. They have a similar energy density to conventional diesel [6]. Pinenes, also known as monoterpenes, are the simplest terpenes and consist of two isoprene building blocks. Two constitutional isomers, i.e., α- and β-pinene, exist, but α-pinene is the more abundant isomer. Both have two stereocenters and overall four enantiomers of the pinenes occur in nature (see Fig. S1 for their structure). A natural source of pinenes is turpentine, which is mainly obtained by tapping pines or as a by-product of papermaking [7].

Previous investigations on the combustion of pinene isomers are limited and focus mainly on the combustion properties of α-pinene. The minimum ignition energies [8] and the laminar burning speeds as well as the Markstein lengths [9] were determined for different α-pinene/benzene/air mixtures. Measurements of minimum ignition energies [10] and laminar burning speeds [11] are also available for α-pinene/air mixtures. It has been reported by Raman et al. that pure α-pinene is suitable for gasoline engines, but observed soot concentrations are higher than those of FACE A and EURO V fuel standards [12].

Early pyrolysis studies of pinenes showed that both α-pinene and β-pinene isomerize to different $C_{10}H_{16}$ species including the acyclic monoterpenes alloocimene from α-pinene and myrcene from β-pinene [13,14]. Burwell published a mechanism explaining the formation of the observed isomerization products during the pyrolysis of pinenes via diradical transition states [14]. Recent studies on the pyrolysis of pinenes show that α-pinene produces mainly alloocimene and limonene and β-pinene mainly limonene, myrcene, and Ψ-limonene via diradical transition states [15,16]. Figure 1 shows the structural formulas of $C_{10}H_{16}$ isomers formed during pyrolysis of pinenes by opening the four-membered ring in the pinene molecule. The monocyclic terpenes are formed by hydrogen shift reaction from the biradicals, while formation of the acyclic terpenes needs C-C bond scission and intramolecular radical recombination [15]. For alloocimene, fast isomerization from the acyclic β-ocimene is assumed [16].

In this work, the first quantitative speciation dataset of combustion intermediates from flat premixed low-pressure flames with α- and β-pinene as fuel are shown. Moreover, the combustion of myrcene, which is considered as the main pyrolysis product of β-pinene, was investigated. Chemical structures of the three investigated $C_{10}H_{16}$ monoterpenes are shown in Fig. 1.

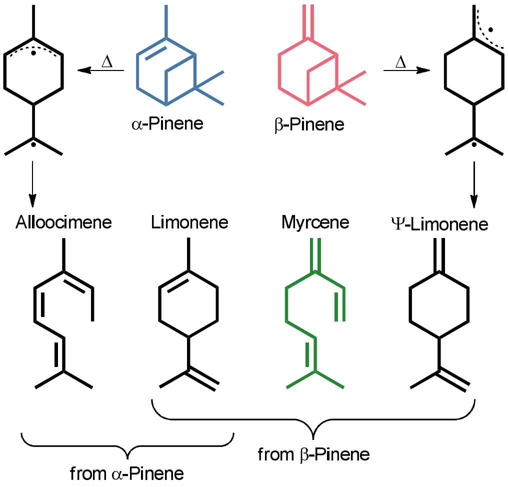

Fig. 1. Isomeric main products in pyrolysis of α- and β-pinene formed by diradical transition states.

## 2. Experiment

Three stoichiometric (Φ=1.0), flat premixed flames of the three $C_{10}H_{16}$ isomers (-)-α-pinene (Sigma-Aldrich, ≥97%), (-)-β-pinene (Sigma-Aldrich, ≥97%), and myrcene (Sigma-Aldrich, ≥95%) were investigated at the Advanced Light Source. The total gas flow was 4 slm (2 slm Ar, 1.867 slm $O_2$, and 0.133 slm $C_{10}H_{16}$) with a cold gas velocity of 87.5 cm/s at 300 K for all three flames. Flames were stabilized at 30 mbar on a McKenna burner with a sintered stainless steel matrix 6 cm in diameter. Table S1 summarizes the flame conditions. The photoionization molecular-beam mass spectrometry experiment is described in detail in [17] and in the supplementary material. The data evaluation process to obtain species mole fraction profiles is also described in the supplementary material. Energy resolution was 50 meV for all measured photoionization efficiency (PIE) spectra. Uncertainty of calculated species mole fractions is estimated to be 15–20% for main species, 30–50% for intermediate species with measured photoionization cross sections (PICS), and a factor of 2–4 for species with unknown PICS. Species with unknown PICS were quantified from scans not more than 0.5 eV above their ionization energy so that their estimated PICS from chemically similar species are typically between 5–10 Mb. Uncertainties in flame-sampling MBMS were further discussed in [18]. Exhaust gas temperatures were measured in the flames with a type R thermocouple coated with $SiO_2$ to minimize catalytic effects. Temperature profiles were determined from the temperature dependence of the sampling rate through the sampling nozzle [19]. Uncertainty of the temperature profiles is expected to be 5–10%.

## 3. Results

Understanding of the combustion chemistry of monoterpenes becomes of scientific importance due to the increasing interest in biomass-derived, alternative fuels. To gain fundamental knowledge about the decomposition of the three monoterpenes, i.e., α-pinene, β-pinene, and myrcene, and the formation of combustion intermediates, flames are compared with each other. The isomer-resolved speciation data can also be used as a starting point for future mechanism development and validation.

### 3.1 Major species

The three investigated fuels have the same elemental composition, i.e., $C_{10}H_{16}$, and the input composition of the gas phase mixtures is identical for all three flames. With similar heating values, the exhaust gas temperatures and the exhaust gas concentrations of the major species should be nearly equal. The heats of combustion of several terpenes including the three investigated monoterpenes of this study were determined by Hawkins and Eriksen [20]. The values at standard conditions are 1483.0 kcal/mol for α-pinene, 1485.1 kcal/mol for β-pinene, and 1490.4 kcal/mol for myrcene [20] and are therefore close to each other. For comparison, volumetric heat of combustion of JP-10, practically a single-component fuel (*exo*-tetrahydrodicyclopentadiene) and an isomer of the three investigated terpenes, is about 7% higher than for the pinenes [3].

Profiles of the major species (Ar, $H_2$, $H_2O$, CO, $CO_2$, $O_2$, and fuel) were determined experimentally for the stoichiometric α-pinene, β-pinene, and myrcene flames (for data, see supplementary material). As expected, the mole fraction profiles are very similar for all three isomers and measured exhaust gas temperatures only differ by 20 K. Differences in the exhaust gas concentrations at 30 mm are below 10% except for hydrogen, whose mole fraction is very small compared to the mole fraction of $H_2O$ (ratio of about 1:10). Deviations in the mole fraction of $H_2O$, which are within the error margin of the equivalence ratio set by thermal mass flow controllers, lead to significant deviations of the hydrogen mole fraction, when calculated from the element balance. A small difference is observed for the mole fraction profiles of the fuels. α-Pinene degrades at slower rate than β-pinene and myrcene, but all three fuels are completely consumed at HAB of 2.7 mm. In addition, $O_2$ degradation is slightly faster for both pinene isomers compared to myrcene. These differences are within the uncertainty of the experiment, so that the major species mole fraction profiles do not differ significantly. Any differences in the reaction kinetics of the fuels are linked to the different fuel destruction pathways and must be deduced from comparison of mole fraction profiles of combustion intermediates.

### 3.2 Unimolecular dissociation of myrcene and comparison of species pool

More than 50 combustion intermediates could be quantified in each of the flames and complete speciation datasets are provided as supplementary material. Most of the identified species were detected in all three flames, but in different concentrations. Differences between the two bicyclic pinene isomers are greater than those between β-pinene and the acyclic monoterpene myrcene. For example, distinct differences are observed for some $C_5H_x$ species as shown in Fig. 2. Compared to the α-pinene flame, the concentrations of $C_5H_7$ and $C_5H_9$ radicals in the β-pinene flame are about one order of magnitude higher. Concentrations of both radicals are even higher in the myrcene flame. It is obvious that the observed differences in the formation of $C_5H_7$ and $C_5H_9$ radicals may be directly related to the first fuel decomposition steps.

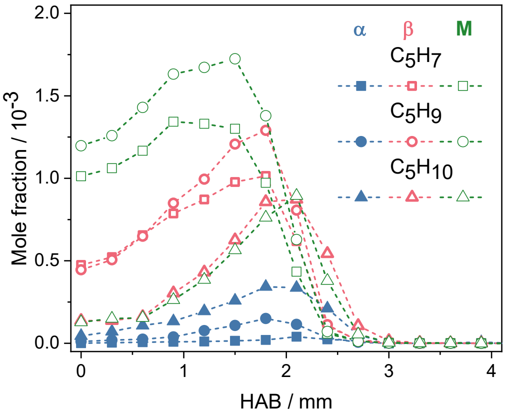

Fig. 2. Mole fraction profiles of $C_5H_x$ species measured in stoichiometric terpene flames. Blue symbols: α-Pinene (α); Red symbols: β-Pinene (β); Green symbols: Myrcene (M).

Myrcene is an acyclic terpene with three types of C-H bonds and H-abstraction is principally possible at the vinylic, allylic or primary carbon atoms. Figure 3 shows the three types of carbon atoms in myrcene. Hydrogen abstraction at the allylic carbon atoms is most likely because the allylic C-H bond is the weakest C-H bond in myrcene. According to Blanskby and Ellison, the bond dissociation energy of an allylic C-H bond is only 88.8 kcal/mol, which is much smaller than for a vinylic (110.7 kcal/mol) or primary (104.9 kcal/mol) C-H bond [21]. A systematic study of H-abstraction ratios for simple hydrocarbons shows that this order of bond strengths is also relevant in flat premixed flames [22]. H-abstraction reactions followed by β-scissions cannot explain the formation of the $C_5H_7$ or the $C_5H_9$ radical in myrcene combustion.

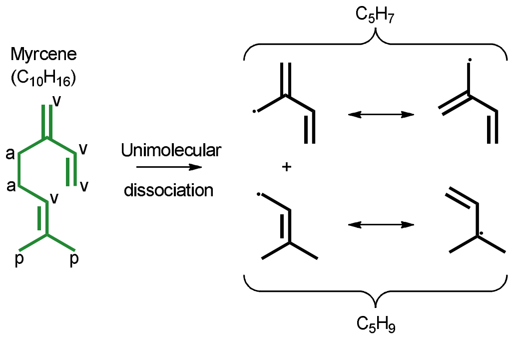

Fig. 3. Labeling of vinylic (v), allylic (a), and primary (p) carbon atoms in myrcene and scheme for the formation of resonance-stabilized $C_5H_7$ and $C_5H_9$ radicals by unimolecular dissociation of myrcene.

In the combustion of higher alkenes, unimolecular cleavage of C-C single bonds in allylic position plays a role and is a common decomposition pathway of the fuel. Hansen et al. showed that the unimolecular C-C bond breaking in 1-hexene to directly form allyl and *n*-propyl radicals is the most important decomposition pathway in flames [23]. In the high-temperature oxidation of alkenes, a C-C bond cleavage typically results in the formation of a resonance-stabilized radical and an alkyl radical [24]. For myrcene, only the cleavage of one C-C single bond leads directly to $C_5H_7$ and $C_5H_9$ radicals (see Fig. 3) and can explain the high concentrations of these radicals in the myrcene flame. Cleavage of this C-C bond is very likely because both of the radicals are resonance-stabilized. Stolle and Ondruschka also proposed a unimolecular bond breaking in the pyrolysis of myrcene [25]. The radicals shown in Fig. 3 are 2-methylene-3-butenyl ($C_5H_7$) and 3-methyl-1-buten-3-yl ($C_5H_9$). Measured photoionization efficiency (PIE) spectra of $C_5H_7$ and $C_5H_9$ from the three terpene flames are shown in Fig. S3. Shape of the PIE spectra of $C_5H_7$ is nearly identical for all flames in the range of 7.9–10 eV, but signal intensity for α-pinene is more than a factor of 10 smaller compared to the other two fuels. The onset in signal intensity at 7.9 eV fits to the estimated ionization energy (IE) of 7.9 eV for the resonance-stabilized 2-methylene-3-butenyl radical [26]. Ionization energies of other $C_5H_7$ isomers are less than 7.6 eV [26], so that their presence can be excluded. PIE spectra of $C_5H_9$ from 7.9–10 eV are shown in Fig. S3. The onset is below 7.9 eV preventing an exact determination of the IE. The 3-methyl-1-buten-3-yl radical has an IE of 7.13 eV [26] and formation is likely as discussed. Shapes of the PIE spectra are again nearly the same in all three flames. It can be assumed that the same radical pool is formed, but that concentrations between the two pinenes may be considerably different.

It seems plausible that mole fractions of the $C_5H_x$ radicals are significantly smaller in the α-pinene flame compared to myrcene since the direct formation of $C_5H_7$ or $C_5H_9$ radicals from the fuel is not expected due to the bicyclic structure. One would expect the same for β-pinene, which also has a bicyclic structure. For both fuels, significantly higher concentrations were observed in comparison to α-pinene, so that it can be concluded that the fuel decomposition of β-pinene differs significantly from α-pinene and there are more similarities to myrcene. There are several other $C_3$–$C_6$ species whose concentrations differ between the two pinene flames, while more similarities are observed between β-pinene and myrcene. Figure 4 compares the maximum mole fractions of eight combustion intermediates from the three flames including the previously discussed $C_5H_7$ and $C_5H_9$ radicals. Because photoionization cross sections for these radicals as well as for $C_4H_5$ are not known, estimated values are used for quantification. Since profile shapes of the PIE spectra for these radicals are very similar in all flames and quantification was done from scans with the same photon energy, comparability of the mole fractions is still given. Stable intermediates from Fig. 4 are, e.g., allene ($aC_3H_4$), 1,2,3-butatriene ($C_4H_4$), and isoprene ($C_5H_8$). Their formation is discussed below, but comparison of the maximum mole fractions further confirms that the species pool formed in the β-pinene flame is more equal to myrcene than to α-pinene. This observation might indicate that β-pinene isomerizes to myrcene during combustion in a flame as seen in pyrolysis where myrcene is a major product besides *p*-mentha-1,8-diene (limonene) and *p*-mentha-1(7),8-diene (ψ-limonene) [15].

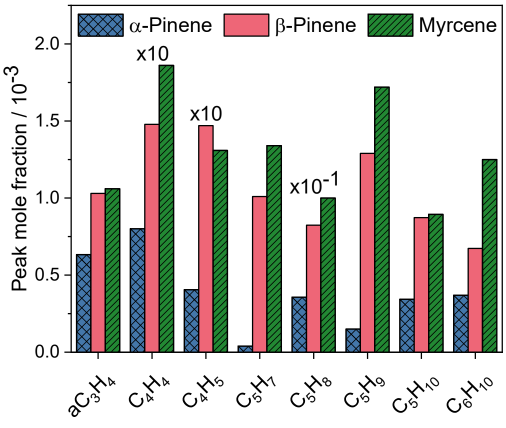

Fig. 4. Peak mole fractions of $C_3$–$C_6$ combustion intermediates measured in α-pinene, β-pinene, and myrcene flames.

### 3.3 Isomerization of the pinenes

Figure 5 compares PIE curves of $C_{10}H_{16}$ obtained at HAB of 2.1 mm (α- and β-pinene) and 1.8 mm (myrcene) in the reaction zone of the terpene flames with the fragmentation scans of the pure substances. Pure substances were vaporized at 180°C, i.e., just above the boiling point, and diluted with argon. Isomerization can be excluded at these conditions. In pyrolysis, the isomerization of α- and β-pinene starts at 300°C [16] and 350°C [15], respectively. Measured ionization energies of 8.15 eV for α-pinene and 8.45 eV for β-pinene agree well with the known values of 8.07 eV [27] and 8.45 eV [28] from the literature. The observed adiabatic IE of myrcene at 8.35 eV is lower than for β-pinene. Similar differences are known for the vertical ionization energies of these two terpenes. Sabljic and Güsten measured vertical ionization energies of 8.61 eV for myrcene and 8.68 eV for β-pinene, respectively [29].

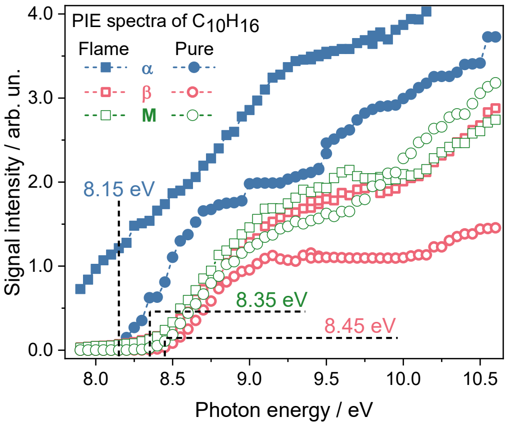

Fig. 5. Comparison of photoionization efficiency (PIE) spectra of $C_{10}H_{16}$ obtained from the three terpene flames with the pure substances. Blue symbols: α-Pinene (α); Red symbols: β-Pinene (β); Green symbols: Myrcene (M).

It is obvious that the onset of the PIE spectrum of $C_{10}H_{16}$ measured in the α-pinene flame is below 7.9 eV, which is significantly smaller than the IE of pure α-pinene. There is also no clear increase in the PIE spectrum at the ionization energy of α-pinene. Complete isomerization of α-pinene seems to be relevant at least at this position in the flame. In the pyrolysis of α-pinene, the main products of isomerization above 300°C are the acyclic alloocimene and the monocyclic limonene (see Fig. 1). Méjean et al. measured ionization energies of several monoterpenes by atmospheric pressure photoionization (APPI) at the SOLEIL synchrotron in France and determined an IE of 8.54 eV for limonene [30]. This value is significantly higher than the IE of α-pinene and there is also no increase in the measured PIE spectrum at this photon energy, which would indicate the formation of limonene in the flame. Adiabatic ionization energies of several diastereomeric structures of alloocimene are located between 7.32 and 7.66 eV at the G4 level of theory (see Table S2) and were calculated with Gaussian 16 [31]. The calculations show that alloocimene has a lower IE than α-pinene and this terpene would be a plausible isomerization product of α-pinene as known from pyrolysis experiments [16]. A few species with mass-to-charge ratio larger than α-pinene, e.g., $C_{11}$ species, are observed in the flame. Since their ionization energies are higher than 7.9 eV, they cannot contribute to the signal of $C_{10}H_{16}$ below 7.9 eV in Fig. 5.

A further species, which may be formed by isomerization of α-pinene, is α-phellandrene. Kolicheski et al. observed the formation of β-phellandrene during the pyrolysis of β-pinene [32] and a possible explanation for the formation of this species was given by Stolle and Ondruschka, who proposed a sigmatropic [1,3]-H-shift from the diradical structure after ring opening of β-pinene [25]. In analogy to β-pinene, α-phellandrene could be formed from α-pinene. A vertical ionization energy of 7.79 eV was calculated by Nauduri and Greenberg [33]. Thus, α-phellandrene would be a second terpene that has a lower IE than α-pinene and may be formed under our flame conditions. The observations suggest that unimolecular isomerization of α-pinene is an important fuel consumption pathway in flames. Fuel consumption by unimolecular isomerization under ring opening was also identified as important decomposition step in methylcyclohexane flames [34].

PIE spectra of $C_{10}H_{16}$ from β-pinene and myrcene flames are very similar as shown in Fig. 5 and the PIE spectrum of pure myrcene fits to these spectra in the measured range, while the PIE spectrum of the pure β-pinene significantly changes near 8.9 eV. Based on these observations, an isomerization of β-pinene to the acyclic myrcene during its combustion can be assumed. The unimolecular decomposition of myrcene discussed before also explains the high concentrations of $C_5H_7$ and $C_5H_9$ radicals in the β-pinene flame. A small onset below the ionization energy of myrcene is observed in the myrcene flame and a possible explanation might be the formation of small amounts of $C_{10}H_{16}$ isomers by H-addition and subsequent C-H-β-scission from myrcene to yield β-ocimene or α-myrcene.

### 3.4 Decomposition of $C_5H_7$ and $C_5H_9$ radicals

A scheme for further decomposition of $C_5H_7$ and $C_5H_9$ radicals, which will be relevant for myrcene and β-pinene flames, is shown in Fig. 6. β-Scission of the C-C single bond between the two vinylic carbon atoms in the 2-methylene-3-butenyl radical ($C_5H_7$) leads to allene ($aC_3H_4$) and vinyl radicals ($C_2H_3$). Mole fraction of allene measured in both the β-pinene and myrcene flame is about 1.6 times higher than for the α-pinene flame. For 3-methyl-1-buten-3-yl radicals ($C_5H_9$), C-C-β-scission is not possible and C-H-β-scission will lead to the formation of the $C_5H_8$ isomers 3-methyl-1,2-butadiene and isoprene. Ionization energies of 3-methyl-1,2-butadiene and isoprene are 8.95 and 8.85 eV, respectively [35]. The measured onset in the PIE spectrum of $C_5H_8$ from the β-pinene flame is about 8.8 eV. A comparison of this measured PIE spectrum with PIE spectra of 3-methyl-1,2-butadiene [36] and isoprene [37] from the literature shows that mainly isoprene is formed since the PIE spectrum from the flame is best reproduced by the PIE spectrum of isoprene (see Fig. S4). Although the spectrum of 3-methyl-1,2-butadiene fits up to a photon energy of 9.2 eV, it clearly differs from the measured spectrum at higher energies. Since the shapes of all measured PIE spectra of $C_5H_8$ are identical in all three flames, isoprene is also the major component of all $C_5H_8$ isomers in the myrcene and α-pinene flame. A possible explanation for the absence of 3-methyl-1,2-butadiene might be a very rapid isomerization to isoprene as reported by Ruwe et al. in the combustion of 2-methyl-2-butene, where 3-methyl-1,2-butadiene could be detected, but the concentration of isoprene was 9 times higher [38]. Isomerization to isoprene would be analogous to isomerization of 1,2-butadiene to 1,3-butadiene via 1,2-H-shift [39]. Isoprene is formed in high concentrations in the β-pinene and myrcene flame with peak mole fractions of $8\cdot10^{-3}$ and $1\cdot10^{-2}$, respectively, as shown in Fig. 4. For comparison, the concentration of isoprene in the α-pinene flame is only about 45% of the value in the β-pinene flame.

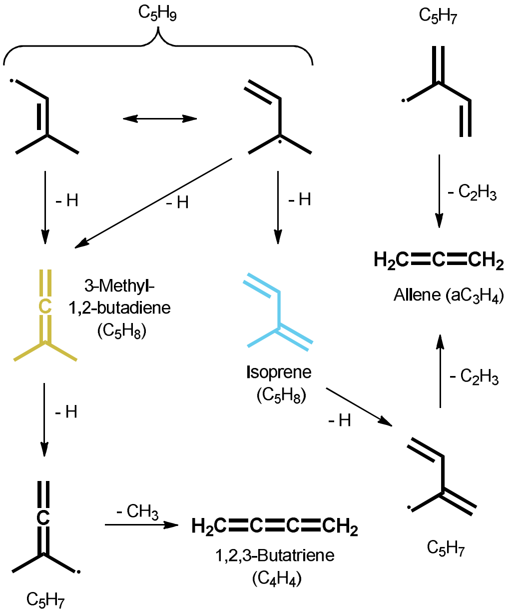

Fig. 6. Scheme for further decomposition of the $C_5H_7$ and $C_5H_9$ radicals.

Starting from 3-methyl-1,2-butadiene and isoprene, another H-abstraction followed by C-C-β-scission leads to 1,2,3-butatriene ($C_4H_4$) or allene ($aC_3H_4$) as shown in the scheme in Fig. 6. The $C_4H_4$ isomer vinylacetylene is the more abundant isomer in all three investigated flames with maximum mole fraction of a factor of 6–8 higher than 1,2,3-butatriene. Since the formation of 3-methyl-1,2-butadiene could not be confirmed, 1,2,3-butatriene is mainly formed as vinylacetylene via $C_4H_5$ radicals [40]. Concentrations of both, 1,2,3-butatriene and the $C_4H_5$ radical, are significantly larger in the β-pinene and myrcene flame. The stable combustion intermediate allene opens additional channels to obtain propyne ($pC_3H_4$) by isomerization and propargyl radicals ($C_3H_3$) by H-abstraction [41].

A competing decomposition pathway of myrcene by H-abstraction reactions is discussed in the supplementary material and shows the formation of $C_{10}H_{14}$, $C_8H_{12}$, $C_4H_5$, and $C_6H_{10}$. Similarities between myrcene and β-pinene for these species are consistent with the isomerization of β-pinene.

### 3.5 Aromatic species and larger hydrocarbons

Figure 7 shows peak mole fractions of $C_3H_7$ radicals and larger $C_8$–$C_{10}$ hydrocarbons from the three terpene flames. Again, results for β-pinene and myrcene are more similar, but maximum mole fractions of shown species are now significantly higher for the α-pinene flame. Aromatic species, e.g., phenylacetylene ($C_8H_6$), styrene ($C_8H_8$), xylenes ($C_8H_{10}$), and indene ($C_9H_8$), were clearly identified by their ionization energies. Larger concentrations of these species indicate that soot formation is potentially higher in the combustion of α-pinene. The mole fraction of benzene is also higher in the α-pinene flame (about a factor of 1.5 compared to β-pinene). During combustion of α-pinene in a gasoline engine, it was also observed that α-pinene even produces more soot than conventional gasoline [12]. The observations made here suggest that β-pinene would be better suited as fuel than α-pinene with respect to avoidance of soot emissions. Other $C_9$–$C_{10}$ hydrocarbons were detected in higher concentrations in the α-pinene flame. However, the ionization energy of the first ionized species of $C_9H_{12}$, $C_9H_{14}$, and $C_{10}H_{14}$ is smaller than the starting point of the energy scan, i.e., smaller than 7.90 eV. If α-phellandrene is an isomerization product during α-pinene combustion as discussed above, its decomposition would lead to *p*-cymene ($C_{10}H_{14}$) after H-abstraction or to the smaller combustion intermediates toluene ($C_7H_8$) and $C_3H_7$.

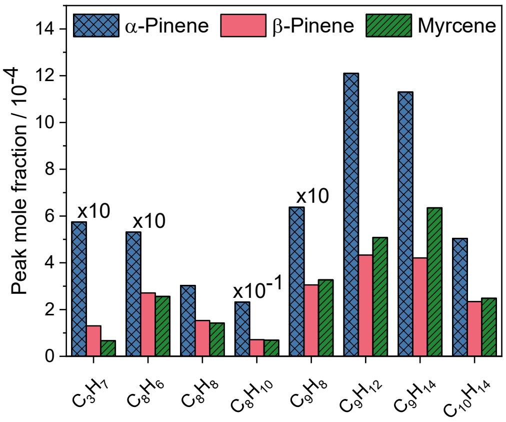

Fig. 7. Peak mole fractions of some combustion intermediates measured in higher concentrations in the α-pinene flame.

Dehydrogenation of the pinenes without ring-breaking, i.e., H-abstraction and subsequent β-scission of a C-H bond, would lead to the formation of the bicyclic verbenene or under cleavage of the $C_4$-ring to substituted cyclohexadienes as shown in Fig. S5 for α-pinene. The formation of substituted cyclohexadienes might be a further explanation for the higher concentrations of aromatic hydrocarbons in the α-pinene flame. For example, Law et al. have demonstrated for a stoichiometric cyclohexane flame that the stepwise dehydrogenation to benzene made a significant contribution to the total benzene concentration [42]. Here, the lack of known ionization energies does not allow further conclusions on the identity of the $C_{10}H_{14}$ species formed in our investigated flames.

## 4. Conclusions

Growing interest in biomass-derived, alternative fuels makes a fundamental understanding of the combustion chemistry of monoterpenes scientifically important, but investigations on the combustion of the pinenes and myrcene are so far limited. In this work, the combustion of the pinene isomers (α- and β-pinene) and myrcene, which is an isomerization product in pyrolysis of β-pinene, were investigated in flat premixed, low-pressure flames at 30 mbar by photoionization molecular-beam mass spectrometry at the Advanced Light Source in Berkeley. More than 50 combustion intermediates formed during combustion of the three studied stoichiometric flames were identified and their mole fractions calculated. The comprehensive speciation data give an insight into the combustion kinetics of the monoterpenes and is made available herein for subsequent model validation. Observed similarities in the species pool between β-pinene and myrcene suggest that β-pinene isomerizes to myrcene during combustion, so that the identified main decomposition steps are the same for both fuels. A detailed decomposition pathway is formulated for myrcene. The speciation data of all three flames provide important information for the development of reaction mechanisms. Given the complexity of the flame chemistry of these fuels and their propensity for isomerization, additional data sets for other possible isomers may be needed to allow meaningful future reaction mechanism development. The most important isomers could be identified and give first experimental evidence for possible reaction pathways that should be included in chemical kinetic modeling. It is also shown that α-pinene isomerizes during combustion, since the formation of a $C_{10}H_{16}$ isomer with significantly lower ionization energy than α-pinene was directly observed. However, the decomposition of α-pinene without previous isomerization needs further investigation, because the clear identification of some larger $C_9$ and $C_{10}$ hydrocarbons was not possible due to unknown ionization energies of candidate compounds. To fully understand the formation of higher aromatic hydrocarbons, it is necessary to determine the ionization energies of possible $C_9$ and $C_{10}$ hydrocarbons. The results show that α-pinene has a higher propensity to form aromatic hydrocarbons and soot. For example, benzene, phenylacetylene, xylenes, styrene and naphthalene were detected in all flames, but the concentrations of all aromatic hydrocarbons are significantly higher in α-pinene under the same conditions. For β-pinene and myrcene, higher levels of unsaturated non-cyclic hydrocarbons were detected, in particular, hydrocarbons having four and five carbon atoms, e.g., 1,3-butadiene and isoprene.

## Acknowledgments

The authors gratefully acknowledge Paul Fugazzi for technical assistance and Patrick Hemberger for calculation of adiabatic ionization energies. TK acknowledges support from the German Research

Foundation (DFG) under contract KA3871/3-2. NH acknowledges support from the U.S. DOE, Office of Science, Office of Basic Energy Sciences. Sandia National Laboratories is a multi-mission laboratory managed and operated by National Technology and Engineering Solutions of Sandia, LLC., a wholly owned subsidiary of Honeywell International, Inc., for the U.S. Department of Energy's National Nuclear Security Administration under contract DE-NA0003525. The experiments were conducted at the Advanced Light Source, Berkeley National Laboratory, Berkeley, CA, USA. The Advanced Light Source is supported by the Director, Office of Science, Office of Basic Energy Sciences, of the U.S. DOE under Contract No. DEAC02-05CH11231.

## References

[1] D. Thrän, K. Naumann, E. Billig, M. Millinger, K. Oehmichen, D. Pfeiffer, K. Zech, in: M.R. Riazi, D. Chiaramonti (Eds.), Biofuels production and processing technology, Taylor & Francis, Boca Raton, 2018, pp. 55-100.

[2] S. Blakey, L. Rye, C.W. Wilson, Aviation gas turbine alternative fuels: A review, Proc. Combust. Inst. 33 (2011) 2863-2885.

[3] B.G. Harvey, M.E. Wright, R.L. Quintana, High-density renewable fuels based on the selective dimerization of pinenes, Energy Fuels 24 (2010) 267-273.

[4] H.A. Meylemans, R.L. Quintana, B.G. Harvey, Efficient conversion of pure and mixed terpene feedstocks to high density fuels, Fuel 97 (2012) 560-568.

[5] H.A. Meylemans, L.C. Baldwin, B.G. Harvey, Low-temperature properties of renewable high-density fuel blends, Energy Fuels 27 (2013) 883-888.

[6] S. Sarria, B. Wong, H.G. Martin, J.D. Keasling, P. Peralta-Yahya, Microbial synthesis of pinene, ACS Synth. Biol. 3 (2014) 466-475.

[7] A. Behr, L. Johnen, Myrcene as a natural base chemical in sustainable chemistry: A critical review, ChemSusChem 2 (2009) 1072-1095.

[8] B. Coudour, K. Chetehouna, S. Rudz, P. Gillard, J.-P. Garo, Investigation on minimum ignition energy of mixtures of α-pinene-benzene/air, J. Hazard. Mater. 283 (2015) 507-511.

[9] B. Coudour, K. Chetehouna, F. Halter, C. Mounaïm-Rousselle, J.-P. Garo, Effects of temperature and equivalence ratio on laminar burning speeds of α-pinene/benzene/air mixtures for different fuel proportions, Combust. Sci. Technol. 188 (2016) 2128-2136.

[10] S. Rudz, K. Chetehouna, C. Strozzi, P. Gillard, Minimum ignition energy measurements for α-pinene/air mixtures, Combust. Sci. Technol. 186 (2014) 1597-1605.

[11] L. Courty, K. Chetehouna, F. Halter, F. Foucher, J.-P. Garo, C. Mounaïm-Rousselle, Experimental determination of emission and laminar burning speeds of α-pinene, Combust. Flame 159 (2012) 1385-1392.

[12] V. Raman, V. Sivasankaralingam, R. Dibble, S.M. Sarathy, α-Pinene - A high energy density biofuel for SI engine applications, SAE Tech. Pap. (2016) 2016-01-2171.

[13] L.A. Goldblatt, S. Palkin, Vapor phase thermal isomerization of α- and β-pinene, J. Am. Chem. Soc. 63 (1941) 3517-3522.

[14] R.L. Burwell, The Mechanism of the pyrolyses of pinenes, J. Am. Chem. Soc. 73 (1951) 4461-4462.

[15] A. Stolle, C. Brauns, M. Nüchter, B. Ondruschka, W. Bonrath, M. Findeisen, Thermal behaviour of selected $C_{10}H_{16}$ monoterpenes, Eur. J. Org. Chem. (2006) 3317-3325.

[16] A. Stolle, B. Ondruschka, M. Findeisen, Mechanistic and kinetic insights into the thermally induced rearrangement of α-pinene, J. Org. Chem. 73 (2008) 8228-8235.

[17] T.A. Cool, A. McIlroy, F. Qi, P.R. Westmoreland, L. Poisson, D.S. Peterka, M. Ahmed, Photoionization mass spectrometer for studies of flame chemistry with a synchrotron light source, Rev. Sci. Instrum. 76 (2005) 094102.

[18] T. Bierkandt, P. Hemberger, P. Oßwald, D. Krüger, M. Köhler, T. Kasper, Flame structure of laminar premixed anisole flames investigated by photoionization mass spectrometry and photoelectron spectroscopy, Proc. Combust. Inst. 37 (2019) 1579-1587.

[19] U. Struckmeier, P. Oßwald, T. Kasper, L. Böhling, M. Heusing, M. Köhler, A. Brockhinke, K. Kohse-Höinghaus, Sampling probe influences on temperature and species concentrations in molecular beam mass spectroscopic investigations of flat premixed low-pressure flames, Z. Phys. Chem. 223 (2009) 503-537.

[20] J.E. Hawkins, W.T. Eriksen, Physical and thermodynamic properties of terpenes. II. The heats of combustion of some terpene hydrocarbons, J. Am. Chem. Soc. 76 (1954) 2669-2671.

[21] S.J. Blanksby, G.B. Ellison, Bond dissociation energies of organic molecules, Acc. Chem. Res. 36 (2003) 255-263.

[22] D. Krüger, P. Oßwald, M. Köhler, P. Hemberger, T. Bierkandt, Y. Karakaya, T. Kasper, Hydrogen abstraction ratios: A systematic iPEPICO spectroscopic investigation in laminar flames, Combust. Flame 191 (2018) 343-352.

[23] N. Hansen, W. Li, M.E. Law., T. Kasper, P.R. Westmoreland, B. Yang, T.A. Cool, A. Lucassen, The importance of fuel dissociation and propargyl + allyl association for the formation of benzene in a fuel-rich 1-hexene flame, Phys. Chem. Chem. Phys. 12 (2010) 12112-12122.

[24] M. Mehl, G. Vanhove, W.J. Pitz, E. Ranzi, Oxidation and combustion of the n-hexene isomers: A wide range kinetic modeling study, Combust. Flame 155 (2008) 756-772.

[25] A. Stolle, B. Ondruschka, Comment to the paper "Synthesis of myrcene by pyrolysis of β-pinene: Analysis of decomposition reactions" by M.B. Kolicheski et al. [J. Anal. Appl. Pyrol. 80 (2007) 92–100], J. Anal. Appl. Pyrolysis 81 (2008) 136-138.

[26] F.P. Lossing, J.C. Traeger, Free radicals by mass spectrometry XLVI. Heats of formation of $C_5H_7$ and $C_5H_9$ radicals and cations, Int. J. Mass Spectrom. Ion Phys. 19 (1976) 9-22.

[27] M.I. Al-Joboury, D.W. Turner, Molecular photoelectron spectroscopy. Part II. A summary of ionization potentials, J. Chem. Soc. (1964) 4434-4441.

[28] M. Cao, J. Chen, W. Fang, Y. Li, S. Ge, X. Shan, F. Liu, Y. Zhao, Z. Wang, L. Sheng, Dissociative photoionization of β-pinene: An experimental and theoretical study, Eur. J. Mass Spectrom. 20 (2014) 419-428.

[29] A. Sabljic, H. Güsten, Predicting the night-time $NO_3$ radical reactivity in the troposphere, Atmospheric Environ. 24 (1990) 73-78.

[30] M. Méjean, A. Giuliani, A. Brunelle, D. Touboul, Determination of ionization energies of a monoterpene series by atmospheric pressure photoionization using tunable vacuum ultraviolet synchrotron radiation, Eur. J. Mass Spectrom. 20 (2014) 403-407.

[31] M.J. Frisch, G.W. Trucks, H.B. Schlegel, G.E. Scuseria, M.A. Robb, J.R. Cheeseman, G. Scalmani, V. Barone, G.A. Petersson, H. Nakatsuji, X. Li, M. Caricato, A.V. Marenich, J. Bloino, B.G. Janesko, R. Gomperts, B. Mennucci, H.P. Hratchian, J.V. Ortiz, A.F. Izmaylov, J.L. Sonnenberg, D. Williams-Young, F. Ding, F. Lipparini, F. Egidi, J. Goings, B. Peng, A. Petrone, T. Henderson, D. Ranasinghe, V.G. Zakrzewski, J. Gao, N. Rega, G. Zheng, W. Liang, M. Hada, M. Ehara, K. Toyota, R. Fukuda, J. Hasegawa, M. Ishida, T. Nakajima, Y. Honda, O. Kitao, H. Nakai, T. Vreven, K. Throssell, J.A. Montgomery, J.E. Peralta, F. Ogliaro, M.J. Bearpark, J.J. Heyd, E.N. Brothers, K.N. Kudin, V.N. Staroverov, T.A. Keith, R. Kobayashi, J. Normand, K. Raghavachari, A.P. Rendell, J.C. Burant, S.S. Iyengar, J. Tomasi, M. Cossi, J.M. Millam, M. Klene, C. Adamo, R. Cammi, J.W. Ochterski, R.L. Martin, K. Morokuma, O. Farkas, J.B. Foresman, D.J. Fox, Gaussian 16, Revision A.03, Gaussian, Inc., Wallingford, CT, 2016.

[32] M.B. Kolicheski, L.C. Cocco, D.A. Mitchell, M. Kaminski, Synthesis of myrcene by pyrolysis of β-pinene: Analysis of decomposition reactions, J. Anal. Appl. Pyrolysis 80 (2007) 92-100.

[33] D. Nauduri, A. Greenberg, Calculated ionization energies for a series of sesquiterpenes: Comparisons with experimental vertical ionization energies and comments on related structure-activity relationships (SARs), Struct. Chem. 20 (2009) 417-421.

[34] S.A. Skeen, B. Yang, A.W. Jasper, W.J. Pitz, N. Hansen, Chemical structures of low-pressure premixed methylcyclohexane flames as benchmarks for the development of a predictive combustion chemistry model, Energy Fuels 25 (2011) 5611-5625.

[35] G. Bieri, F. Burger, E. Heilbronner, J.P. Maier, Valence ionization energies of hydrocarbons, Helv. Chim. Acta 60 (1977) 2213-2233.

[36] B. Yang, J. Wang, T.A. Cool, N. Hansen, S. Skeen, D.L. Osborn, Absolute photoionization cross-sections of some combustion intermediates, Int. J. Mass Spectrom. 309 (2012) 118-128.

[37] X. Liu, W. Zhang, Z. Wang, M. Huang, X. Yang, L. Tao, Y. Sun, Y. Xu, X. Shan, F. Liu, L. Sheng, Dissociative photoionization of isoprene: Experiments and calculations, J. Mass Spectrom. 44 (2009) 404-409.

[38] L. Ruwe, K. Moshammer, N. Hansen, K. Kohse-Höinghaus, Consumption and hydrocarbon growth processes in a 2-methyl-2-butene flame, Combust. Flame 175 (2017) 34-46.

[39] R.D. Kern, H.J. Singh, C.H. Wu, Thermal decomposition of 1,2-butadiene, Int. J. Chem. Kinet. 20 (1988) 731-747.

[40] J.M. Ribeiro, A.M. Mebel, Reaction mechanism and product branching ratios of the CH + $C_3H_4$ reactions: A theoretical study, Phys. Chem. Chem. Phys. 19 (2017) 14543-14554.

[41] N. Hansen, J.A. Miller, P.R. Westmoreland, T. Kasper, K. Kohse-Höinghaus, J. Wang, T.A. Cool, Isomer-specific combustion chemistry in allene and propyne flames, Combust. Flame 156 (2009) 2153-2164.

[42] M.E. Law, P.R. Westmoreland, T.A. Cool, J. Wang, N. Hansen, C.A. Taatjes, T. Kasper, Benzene precursors and formation routes in a stoichiometric cyclohexane flame, Proc. Combust. Inst. 31 (2007) 565-573.

**List of supplemental material:**

PDF document includes supporting tables and figures, discussion of an alternative decomposition pathway of myrcene by H-abstraction reactions, a detailed description of the experiment, and the procedure for the data reduction.

An Excel sheet includes the experimental temperature profiles and mole fraction profiles of the three terpene flames.

**List of figure captions:**

Fig. 1. Isomeric main products in pyrolysis of α- and β-pinene formed by diradical transition states.

Fig. 2. Mole fraction profiles of $C_5H_x$ species measured in stoichiometric terpene flames. Blue symbols: α-Pinene (α); Red symbols: β-Pinene (β); Green symbols: Myrcene (M).

Fig. 3. Labeling of vinylic (v), allylic (a), and primary (p) carbon atoms in myrcene and scheme for the formation of resonance-stabilized $C_5H_7$ and $C_5H_9$ radicals by unimolecular dissociation of myrcene.

Fig. 4. Peak mole fractions of $C_3$–$C_6$ combustion intermediates measured in α-pinene, β-pinene, and myrcene flames.

Fig. 5. Comparison of photoionization efficiency (PIE) spectra of $C_{10}H_{16}$ obtained from the three terpene flames with the pure substances. Blue symbols: α-Pinene (α); Red symbols: β-Pinene (β); Green symbols: Myrcene (M).

Fig. 6. Scheme for further decomposition of the $C_5H_7$ and $C_5H_9$ radicals.

Fig. 7. Peak mole fractions of some combustion intermediates measured in higher concentrations in the α-pinene flame.